Enhanced late Miocene chemical weathering and altered precipitation patterns in the watersheds of the Bay of Bengal recorded by detrital clay radiogenic isotopes

Lisa Bretschneider[1], Ed C. Hathorne[1]*, Clara T. Bolton[2], Daniel Gebregiorgis[3], Liviu Giosan[4], Emmeline Gray[2,5], Huang Huang[1,6], Ann Holbourn[7], Wolfgang Kuhnt[7] and Martin Frank[1]

1 GEOMAR Helmholtz Centre for Ocean Research Kiel, Germany

2 Aix Marseille Univ, CNRS, IRD, INRAE, Coll France, CEREGE, Aix-en-Provence, France

3 Department of Geosciences, Georgia State University, Atlanta, USA

4 Woods Hole Oceanographic Institution, Woods Hole, USA

5 The Open University, Milton Keynes, UK

6 Sun Yat-Sen University, Guangzhou, China

7 Institute of Geosciences, Christian-Albrechts-University Kiel, Germany

* Corresponding author: ehathorne@geomar.de

Contents of this file

Additional Supporting Information (Files uploaded separately)

Dataset S1: Radiogenic Sr, Nd, and Pb isotope composition of clay sized silicate fraction of the late Miocene section of International Ocean Discovery Program (IODP) Site U1443

Dataset S2: Stable carbon isotope composition of benthic foraminifera *C. wuellerstorfi* of the late Miocene section of International Ocean Discovery Program (IODP) Site U1443

Text S1. Detailed methods

Our study is based on sediments drilled at IODP Site U1443 (Latitude 5°23'N; Longitude 90°21'E, water depth ~2930 mbsl) with the RV JOIDES Resolution during IODP Expedition 353 in December 2014. Site U1443 was a redrill of nearby Ocean Drilling Program Site 758 and located on the crest of the Ninetyeast Ridge in the southern Bay of Bengal. This ridge-top location ensured a slow and continuous sedimentation and prevented the deposition of disturbed sedimentary sequences typically associated with transport processes of the Bengal Fan (Clemens et al., 2016). The sedimentation rate during the late Miocene varied between 0.54 and 1.97 cm/kyr and was on average 1.36 kyr/cm. Four holes were combined to form a splice comprising sediments from the Oligocene to the late Pleistocene. The recovered late Miocene sediment comprises the lowermost part of lithogenic unit Ib and is a nannofossil ooze with varying abundances of detrital clays, biosilica, volcanic ash and foraminifers (Clemens et al., 2016). The late Miocene samples span a composite core depth from 70 m to 123 m. The age model used in this study is based on minimal tuning of $\delta13C$ data (Figure S1) of monospecific epifaunal benthic foraminifers *Cibicidoides wuellerstorfi* to the high resolution reference record of ODP Site 1146 (Houlbourn et al., 2018; 2021) and is consistent with revised calcareous nannofossil biostratigraphy (Bolton et al, in review) and shipboard magnetostratigraphy (Clemens et al., 2016) (Figure S1).

Bulk sediment samples were washed at CEREGE over a 63 μm sieve and the fine fraction collected. While the coarse fraction was dried and used for micropaleontological work, the fine fraction was centrifuged, oven dried at 50 °C, and sent to GEOMAR where it was processed to isolate clays. Firstly, the fine fraction was leached to remove all authigenic Fe-Mn oxyhydroxides following a procedure modified from Gutjahr et al. (2007) and the first leach was kept for future analysis of the dissolved radiogenic isotope signature of past seawater. Briefly, ~2 g of fine sediment were washed with deionized water, leached step by step with a 0.05M hydroxylamine hydrochloride–15% distilled acetic acid–0.03M Na-EDTA solution, buffered to pH 4 with analytical grade NaOH. To remove all the oxides, the samples were leached in a strong leach solution overnight before being fully decarbonated with 40 % acetic acid (acid was added until no reaction was visible and then some excess). Having been washed again with deionized water, the clay fraction was separated using a centrifuge-based Atterberg method.

For the radiogenic isotope analyses, the clay fraction was then dried at low temperature (<45°C) in an oven. About 100 mg of the dried clays were completely digested using alkaline fusion (NaOH-Na2O2), as described in Bayon et al. (2009) but without addition of TiO2, Fe2O3 or Tm, and then further dissolved in 6 M HCl. To separate and purify Nd, Sr and Pb, standard ion chromatographic procedures were applied (Cohen et al., 1988; Galer and O'Nions, 1989; Pin and Zalduegui, 1997). For Nd, first the REEs (including Nd) were separated using a cation exchange resin (Bio-Rad AG 50W-X8, 200-400 mesh), while most matrix elements were discarded. The Nd was then separated from the other REEs using Ln-spec resin (50-100 μm). Pb and Sr were separated using AG1-X8 (100-200 μm) and Sr-Spec resin, respectively. Sr isotope measurements were performed on a Nu Plasma high-resolution MC-ICP-MS while Nd and Pb isotope analyses were carried out on a Thermo Scientific Neptune Plus MC-ICP-MS at GEOMAR.

Nd isotope ratios were corrected for instrumental mass bias using a 146Nd/144Nd of 0.7219 (Vance and Thirlwall, 2002) and were normalized to the accepted values of the JNdi-1 standard (0.512115; Tanaka et al., 2000). The Nd isotope ratios are reported as $\varepsilon Nd(0)$ values = ((143Nd/144Nd)sample/(143Nd/144Nd)CHUR − 1) x 104 with CHUR

being the Chondritic Uniform Reservoir and $(^{143}Nd/^{144}Nd)_{CHUR}$ = 0.512638 (Jacobsen and Wasserburg, 1980). Procedural blanks for Nd were ≤50 pg and thus below 0.05 % of the total amount of Nd in the samples. Separate digestions and measurements of USGS reference material BHVO-2 (n=8) gave a mean εNd value of 6.75±0.24, which agrees well with the mean value (6.65±0.60) reported by the GeoReM database (Jochum et al., 2016).

The instrumental mass bias of Sr isotopic measurements was corrected using a $^{88}Sr/^{86}Sr$ of 0.1194 (Steiger and Jäger, 1977) and normalized to the NIST SRM 987 $^{87}Sr/^{86}Sr$ of 0.710245. Procedural blanks were an average 50 ng, contributing between 0.6 and 3 % of the total Sr signal. This rather high contribution originated from the use of NaOH and NaO2 for the alkaline fusion. To correct for the blank contributions, samples of the reagents were regularly digested and measured for concentrations (n=15). These were later combined and measured for their isotopic composition. The blank contributions were then removed from the Sr sample signals via mass balance calculations. Repeated digestions and measurements of USGS reference material BHVO-2 (n=12) gave a mean $^{87}Sr/^{86}Sr$ value of 0.70363±0.00013, which is in good agreement with the GeoReM average value of 0.70348±0.00006.

The mass bias correction for the Pb isotope measurements was carried out by doping the samples with the NIST997 Tl standard solution (Pb/Tl ~4) (Belshaw et al., 1998; White et al., 2000). Since Tl and Pb fractionate slightly differently during ionization (Vance and Thirlwall, 2002), $^{205}Tl/^{203}Tl$ was adjusted on a session-by-session basis in order to match accepted SRM 981 Pb isotope compositions ($^{206}Pb/^{204}Pb$ = 16.9416, $^{207}Pb/^{204}Pb$ = 15.4998 and $^{208}Pb/^{204}Pb$ = 36.7249; Baker et al., 2004). Repeated processing and analysis of USGS reference material BHVO-2 (n=6) gave mean values (±2 standard deviations) of 18.619±0.090, 15.536±0.019, and 38.219±0.052 for $^{206}Pb/^{204}Pb$, $^{207}Pb/^{204}Pb$, and $^{208}Pb/^{204}Pb$, respectively. These Pb isotope values agree well with those previously measured for BHVO-2 (n=44, 18.637±0.073, 15.528±0.045, and 38.223±0.103; GeoReM database). Procedural blanks for Pb were ≤60 pg and contributed less than 0.1% of the total amount of Pb in the samples.

Figure S1. Comparison of low resolution IODP Site U1443 *Cibicidoides wuellerstorfi* benthic δ¹³C with the high resolution data from ODP Site 1146 in the South China Sea (Houlborn et al., 2018; in press). High or low points with yellow arrows are marked in the data table to facilitate use as tie points. Shipboard paleomagnetic and nannofossil datums (Clemens et al., 2016) are assigned to the δ¹³C datapoint with the nearest composite depth. The 6.91 Ma datum was refined post cruise by C. Bolton.
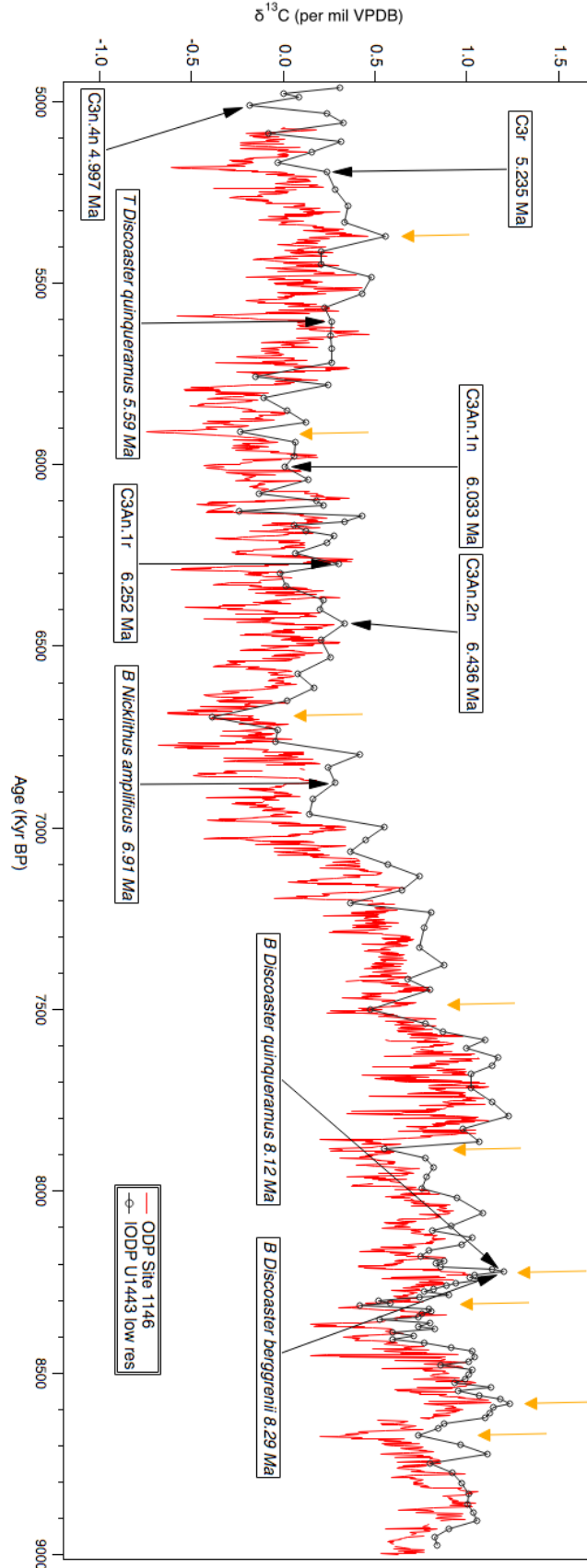
Table S1. Sr, Nd, and Pb average isotopic compositions and concentrations (ug/g) for the major lithologies and river systems used as endmembers from the literature.

Endmember	$^{87}Sr/$ ^{86}Sr	Sr	ε_{Nd}	Nd	$^{206}Pb/$ ^{204}Pb	$^{208}Pb/$ ^{204}Pb	References
IBR	0.71	200	-5.2	24			Awasthi et al. (2014)
TSS	0.727	229	-13	26.7			France-Lanord et al. (1993)
HHC	0.755	70	-15.5	23.6			France-Lanord et al. (1993); Singh and France-Lanord (2002)
LH	0.85	70	-24.4	40.3	21		Singh and France-Lanord (2002); Clift et al. (2002)
TPB	0.705	400	-6.5				Singh and France-Lanord (2002)
Irrawaddy	0.716	100	-6.47	50	18.751	39.098	Awasthi et al. (2014); this study
Brahmaputra	0.719	212	-12.5	35.6	18.938	39.571	Singh and France-Lanord (2002); Millot et al. (2004)
Ganges	0.772	32	-17.2	23.6	19.508	39.766	Singh and France-Lanord (2002); Millot et al. (2004)